ACS OMEGA

Open Access

http://pubs.acs.org/journal/acsodf

Article

Absolute Saturation Vapor Pressures of Three Fatty Acid Methyl Esters around Room Temperature

Mohsen Salimi, Jonas Elm, Aurelien Dantan, and Henrik B. Pedersen*

Cite This: *ACS Omega* 2025, 10, 6671−6678

Read Online

ACCESS | Metrics & More | Article Recommendations | Supporting Information

ABSTRACT: We report measurements of absolute saturation vapor pressures around room temperature for three fatty acid methyl esters (methyl octanoate, methyl decanoate, and methyl dodecanoate) using a recently developed experimental method in which the saturation vapor pressures are determined from the vaporization dynamics of a cooled sample during thermalization to a higher chamber temperature.

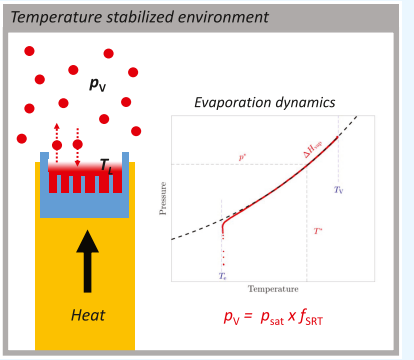

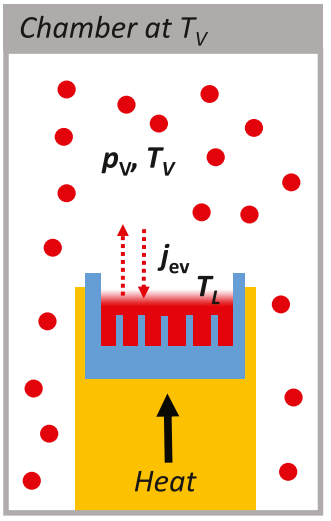

Figure 1. Simplified illustration of the experimental system, showing (i) the sample (red) at the momentary temperature T_L inside a sample holder that is in contact with the surrounding chamber, stabilized at temperature T_V, through a thermal bridge, and (ii) the gas vapor at pressure p_V and temperature T_V above the sample. Due to the largely different time scales of heat transfer from the chamber to the sample (slow) and the response (fast) of the net particle flux j_{ev} (from the sample to the environment) to a temperature change, the value of j_{ev} can be considered equal to zero during the thermalization process. A complete description of the setup and the principle of the analysis has been given recently by Nielsen et al.[23]

1. INTRODUCTION

Fatty acid methyl esters (FAMEs) are among the primary constituents of biodiesel fuels.[1,2] FAMEs occur naturally, for instance, in vegetable oils and animal fats, and they also find use in numerous applications, for example, as base ingredients for chemical synthesis and analysis, for lubrication and coatings, and in health care products; see, e.g., the reviews in refs 2,3. Due to their widespread occurrences and applications, the saturation vapor pressures and enthalpies of vaporization (characterizing the temperature dependence of the vapor pressure) of FAMEs have been of significant interest for several decades.[4−17] The knowledge of saturation vapor pressures and enthalpies of vaporization for FAMEs (along with other thermodynamical properties) can be important for the development of engines using biofuel, for process optimization, e.g., in the pharmaceutical industry, and for food development and processing where FAMEs are, for example, used as flavoring substances.

The first measurements of saturation vapor pressures of FAMEs[4−8] were based on observing the boiling points of liquid samples as a function of ambient pressure. Later, vaporization data for several FAMEs have been obtained[10,12] with techniques based on gas chromatography[10,18] where measurements of the gas concentration from an evaporating substance

Received: September 3, 2024
Revised: December 14, 2024
Accepted: February 6, 2025
Published: February 11, 2025

https://doi.org/10.1021/acsomega.4c08095
ACS Omega 2025, 10, 6671−6678

Table 1. Properties of the Chemical Samples of FAMEs Used in the Present Work

compound name	formula	CAS reg. no.	supplier	purity (%)[b]	method
methyl octanoate	$C_9H_{18}O_2$	CAS 111-11-5	Sigma-Aldrich/Merck	99.9	GC[a]
methyl decanoate	$C_{11}H_{22}O_2$	CAS 110-42-9	Sigma-Aldrich/Merck	99.5	GC[a]
methyl dodecanoate	$C_{13}H_{26}O_2$	CAS 111-82-0	Sigma-Aldrich/Merck	99.5	GC[a]

[a]Gas chromatography. [b]The purity is specified as a percentage of the GC-peak areas.

were related to the saturation vapor pressure. The most recent methods applied to FAMEs are either static measurements[13−16] using devices, see, e.g., refs 13,19, where the absolute pressure above a thermalized sample (inserted in a regulated heat bath) is directly measured, or gas saturation methods (transpiration methods),[16] where the amount of transported material in a gas stream during a definite period of time is recorded.[20,21] The determinations of enthalpies of vaporization of FAMEs have been inferred from the temperature dependencies of the measured saturation vapor pressures and either extrapolated to room temperature using additional measurements of heat capacities[22] or obtained with direct calorimetric methods.[9]

In this paper, we report the measurements of absolute saturation vapor pressures of three FAMEs using a recently realized experimental system and validated method.[23] The applied method is illustrated in Figure 1 and relies on isolating a cooled sample in a clean and static vacuum chamber (no active pumping) and observing the pressure (p_V) in the chamber as a function of the sample temperature (T_L) during the thermalization of the sample toward the chamber temperature (T_V). The central assumption underlying the functioning of the method is that the chamber pressure (p_V) adjusts fast (time scale of seconds) to the liquid temperature (T_L), while the liquid temperature adjusts slowly (time scale of tens of minutes) to the chamber temperature (T_V). Under such conditions, the net particle flux j_{ev} from the sample, balancing vaporization and condensation, is in a steady state ($j_{ev} \approx 0$) throughout the thermalization process, and this steady state condition can then be used to accurately model the vaporization dynamics of the sample by using statistical rate theory. The method has been recently validated through measurements on four reference liquid substances.[23] To ensure an accurate modeling[23] of the experimental results, we have further performed quantum chemical calculations of the vibrational level energies for the three FAMEs.

Using this dynamical method, we report new measurements of the saturation vapor pressure of three FAMEs, namely, methyl octanoate, methyl decanoate, and methyl dodecanoate in ranges (∼20−35 °C (292.15−308.15 K)) around room temperature. For all three studied FAMEs, the previously reported saturation vapor pressures show deviations on the order of 10% or more among each other. The results reported here display very good agreement with some previous results, while disagreements are substantial compared to those of others. The applied method is fundamentally different from the ones used in previous measurements as it relies on observing the system during thermalization, in contrast to static equilibrium condition, and directly gives saturation vapor pressures for the *entirely* probed temperature range. Thus, the new data provided here are complementary to previous measurements and can, for example, be used to qualify the best values for the saturation vapor pressure of the three FAMEs directly around room temperature.

2. EXPERIMENTAL SECTION

2.1. Samples of FAMEs. The properties of the samples used for FAMEs are summarized in Table 1. The samples were

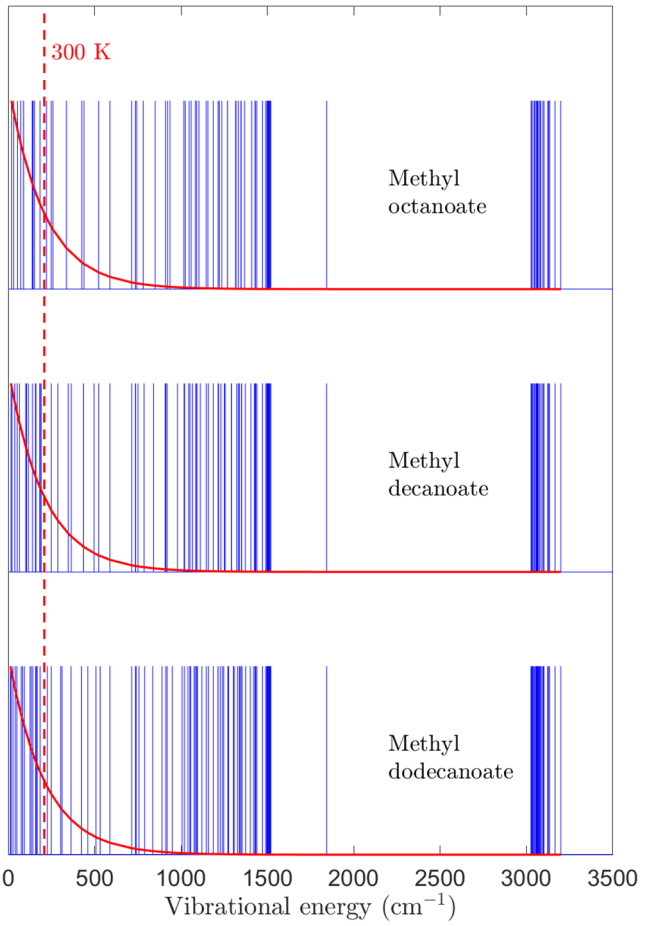

Figure 2. Illustration of the vibrational frequencies for the FAMEs studied. Each blue vertical bar represents a vibrational mode of the specified molecules. The lines at ∼1800 cm^{-1} correspond to vibrations of the carbonyl group. The vertical red dashed lines show the energies corresponding to a temperature of T = 300 K, and the red solid lines show the corresponding relative populations of the vibrational levels, i.e., $f_l = \exp(-(E_l - E_1)/k_BT)$.

Table 2. Determined Number of Conformers for the FAMEs Investigated

molecule	number of conformers
methyl octanoate	770
methyl decanoate	3182
methyl dodecanoate	9889

further purified (removing volatile impurities, i.e., presumably mainly water) by evacuation either at low (evacuation by a scroll pump) or high (evacuation by a turbo pump) vacuum

https://doi.org/10.1021/acsomega.4c08095
ACS Omega 2025, 10, 6671−6678

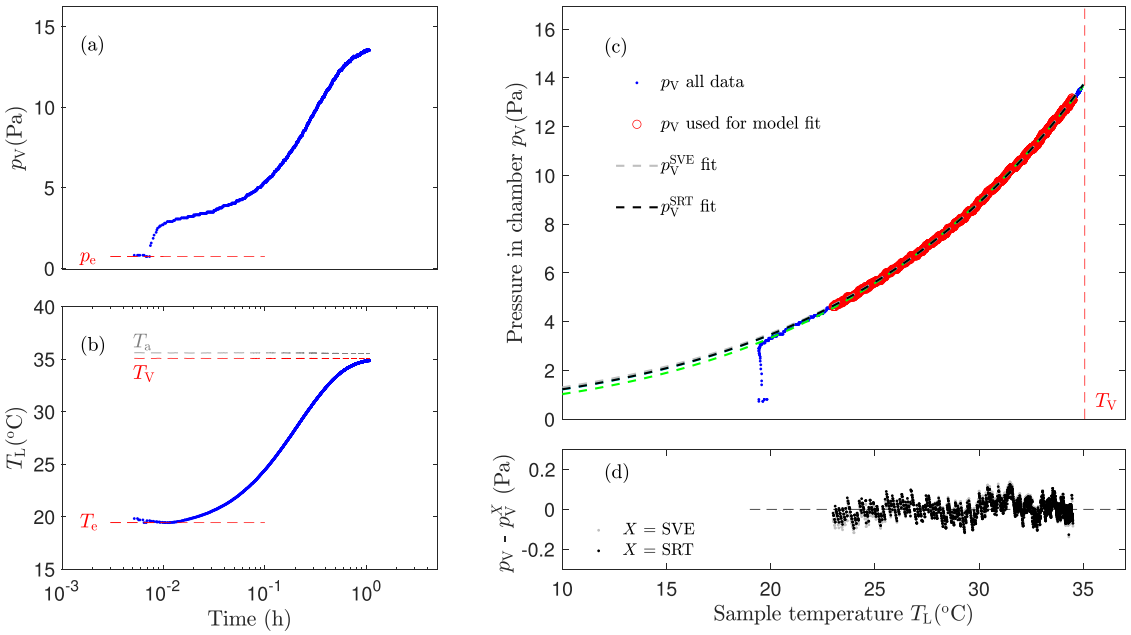

Figure 3. Example of measurements of absolute saturation vapor pressures for methyl decanoate. (a) Pressure in the experimental chamber p_V as a function of time. The indicated pressure p_e is the chamber pressure when the chamber is actively evacuated with the turbo pump. (b) Temperature of the sample (T_L) as a function of time. The temperature T_e is the temperature of the sample obtained due to evaporative cooling. The temperature T_V (=35.0 °C) is the fixed temperature of the chamber. The upper dashed lines marked T_V and T_a show the measured temperatures of the experimental chamber and the ambient air surrounding it, respectively. (c) Chamber pressure as a function of sample temperature showing the full set of experimental data (blue dots) and the data used for modeling (red circles). The dashed curves show fits with the full SRT model[23] and the low-temperature SVE model (eq 4, with $D_e = 0$). See Table 3 for the results of the model fits. (d) Residuals of the data and the model fits.

depending on the actual saturation vapor pressure of the FAME and ensuring that all of the samples should not disappear during evacuation. For methyl octanoate, the purification was done by pumping with the turbo pump for a few minutes, for methyl decanoate by evacuating with a scroll pump for 30 min, followed by 15 min evacuation with a turbo pump, and for methyl dodecanoate by 80 min of continuous evacuation by a turbo pump.

2.2. Dynamical Determination of Saturation Vapor Pressure. Figure 1 illustrates the experimental principles applied in the present measurements. The details of the experimental setup, the analysis procedure, the evaluation of measurement uncertainties, and the validation of the method through comparison of measured saturation vapor pressures of four compounds to reference data have been described in detail in a recent work,[23] and we will therefore not focus on these aspects in this paper, but rather outline the most essential points of the analysis.

Under the condition of a steady state particle flux ($j_{ev} = 0$) from the sample during the thermalization process, the experimentally observed relation of chamber pressure and sample temperature $p_V(T_L)$ can be accurately modeled using statistical rate theory (SRT) for the particle flux.[24−26] Thus, the chamber pressure can be written as[23]

$$p_V^X(T_L) = p_{sat}(T_L) \times f_X(T_L, T_V, \omega_l) \quad (1)$$

where $p_{sat}(T_L)$ is the saturation vapor pressure of the investigated substance at temperature T_L and f_X is a characteristic function that accounts for the vaporization dynamics during thermalization of the sample to the chamber temperature under the condition of a steady particle flux ($j_{ev} = 0$). The function f_X generally depends on the sample and chamber temperatures as well as the vibrational frequencies ω_l (=$E_l/\hbar$, see Section 2.3) of the target molecule. The label for the vibrational levels spans l = 1, ..., DOF, where DOF is the number of vibrational degrees of freedom of the molecule.

For an ideal gas above the liquid sample, the temperature dependence of the saturation vapor pressure is given by the Clausius−Clapeyron equation

$$\frac{dp_{sat}}{dT} = \frac{\Delta H_{vap}}{k_B N_A T^2} \times p_{sat} \quad (2)$$

where ΔH_{vap} is the enthalpy of vaporization, k_B is Boltzmann's constant, and N_A is Avogadro's number. For a temperature-independent ΔH_{vap} in the temperature range of interest, the saturation vapor pressure can be parametrized as

$$p_{sat}(T) = p^* \times \exp\left[-\frac{\Delta H_{vap}}{k_B N_A}\left(\frac{1}{T} - \frac{1}{T^*}\right)\right] \quad (3)$$

where p^* is the saturation vapor pressure at temperature T^*.

The function f_X in eq 1 must generally (X = SRT) be determined numerically from the condition $j_{ev} = 0$,[23] and relies on the explicit knowledge of the substance molecule's vibrational energies. However, the limiting cases of low and high temperatures can be written analytically as

$$p_V^X(T_L, D_e) = p_{sat}(T_L) \times \exp\left[(D_e + 4)\left(1 - \frac{T_V}{T_L}\right)\right]\left(\frac{T_V}{T_L}\right)^{D_e+4} \quad (4)$$

where D_e = DOF in the limit of high temperature (thermal energy dominated limit, X = TED) and $D_e = 0$ in the limit of zero temperature (suppressed vibrational excitation, X = SVE). As demonstrated with the validation of the present method around room temperature,[23] the full statistical rate theory (X =

https://doi.org/10.1021/acsomega.4c08095
ACS Omega 2025, 10, 6671−6678

Table 3. Experimentally Determined Parameters for the Saturation Vapor Pressures for the Three Fatty Acid Methyl Esters Studied[a]

		SRT (complete model)		SVE (low-temperature limit)		
material	T^* (°C (K))	p^* (Pa)	ΔH_{vap} (kJ/mol)	p^* (Pa)	ΔH_{vap} (kJ/mol)	range (°C (K))
methyl octanoate	25.0 (298.15)	50.8 ± 0.4	57.6 ± 0.2 ± 1.2	50.2 ± 0.8	58.6 ± 0.2 ± 1.2	20.0−34.5 (292.15−307.65)
methyl decanoate	25.0 (298.15)	5.7 ± 0.1	66.9 ± 0.3 ± 1.3	5.7 ± 0.1	68.0 ± 0.2 ± 1.3	23.0−34.5 (296.15−307.65)
methyl dodecanoate	25.0 (298.15)	0.63 ± 0.01	75.5 ± 0.3 ± 1.5	0.62 ± 0.01	76.7 ± 0.2 ± 1.4	24.0−34.5 (297.15−307.65)

[a]The saturation vapor pressure in the fully investigated temperature range can be evaluated with eq 3. The results labeled with SRT (statistical rate theory) give the parameters of the saturation vapor pressures obtained with the most accurate modeling. For completeness, the results labeled SVE (suppressed vibrational excitation) give the corresponding parameters obtained with the low-temperature limit of the model, i.e., eq 4 with $D_e = 0$. As seen, the simpler low-temperature model (SVE) gives results in agreement with the complete model (SRT) within the uncertainties. Note that T^* is a fixed (chosen) parameter in the modeling. The specified uncertainties correspond to expanded uncertainties, i.e., representing 95% confidence intervals. The first given errors for values of the enthalpies of vaporization (ΔH_{vap}) reflect the uncertainties obtained from the model fits, and the second given errors reflect the additional uncertainty due to the unmodeled temperature dependence of ΔH_{vap}.[23]

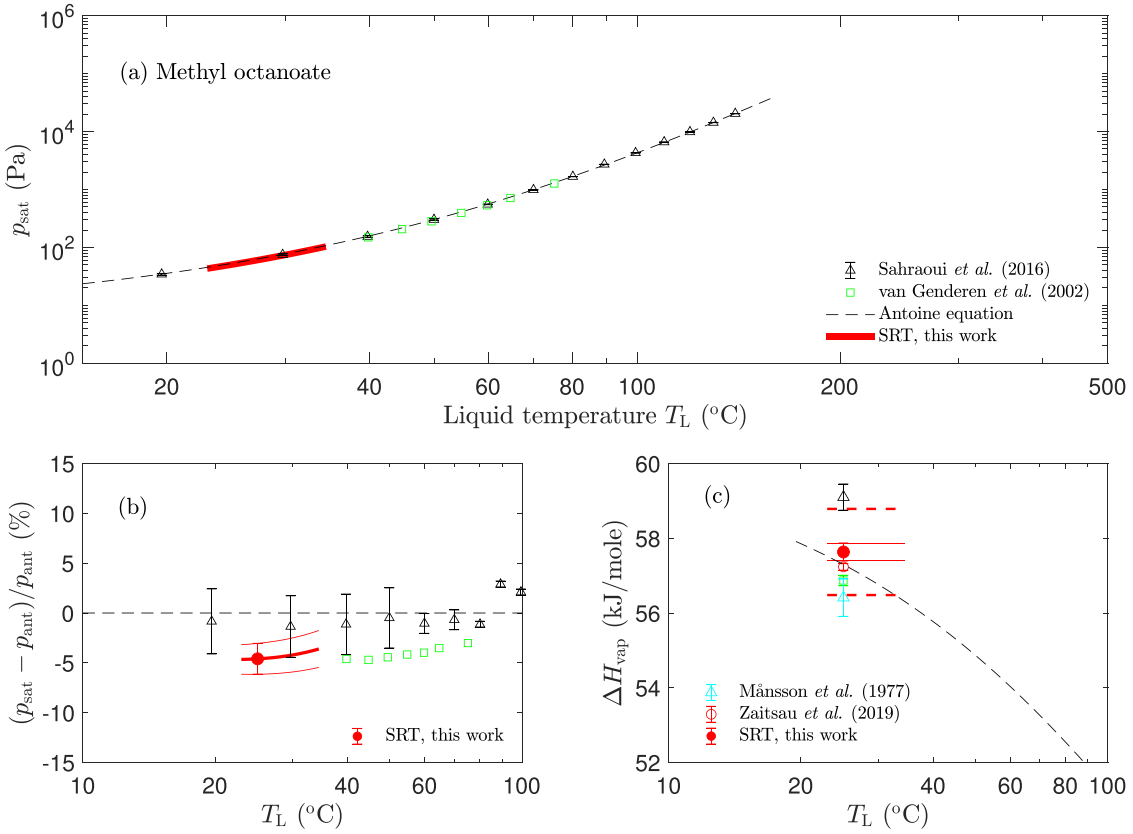

Figure 4. Results of absolute saturation vapor pressure measurements for methyl octanoate and comparison to previous results.[9,14−16] (a) Saturation vapor pressure as a function of sample temperature. The present data is shown as a red solid line following the form of eq 3 with the fitted values of p^* and ΔH_{vap} from the SRT model (f_{SRT}, eq 1) as given in Table 3. The dashed line shows the Antoine equation established by Sahraoui et al.[15] for the temperature range 10−160 °C. (b) Relative comparison of saturation vapor pressures with the Antoine equation.[15] Note that the Antoine equation is extrapolated outside its nominal temperature range. The red solid lines show the 95% confidence interval of the present measurement. (c) Comparison of the present and previously determined enthalpies of vaporization. The solid red lines indicate the uncertainty from the model fits, while the dashed red lines show the additional 2% uncertainty estimated from the unmodeled temperature dependence of ΔH_{vap}.

SRT) as well as the simpler low-temperature model (X = SVE) both provide very good representations of the observed vaporization dynamics during thermalization, while the high-temperature model (X = TED) shows a less satisfactory representation of the experimental $p_V(T_L)$ relation. This is reasonable since at room temperature only a few vibrational levels are populated, as also seen from the explicit calculations shown in Figure 2. For example, for methyl decanoate, the effective number of populated vibration levels can be estimated as $\sum_{l=1}^{DOF} \exp[-(E_l - E_1)/k_B T_L] \approx 10$, which should be compared to DOF = 99 valid in the high-temperature limit.

2.3. Quantum Chemical Computation. Quantum chemical computations were performed on the studied FAMEs to evaluate their spectrum of vibrational frequencies as necessary for the SRT modeling.[23] To study the different conformations of the FAMEs, we employed the Conformer-Rotamer Ensemble Sampling Tool (CREST)[27−29] Version 2.12 to locate the lowest energy conformer. We used the GFN1-xTB model[30] in the CREST run calculated with the xtb

https://doi.org/10.1021/acsomega.4c08095
ACS Omega 2025, 10, 6671−6678

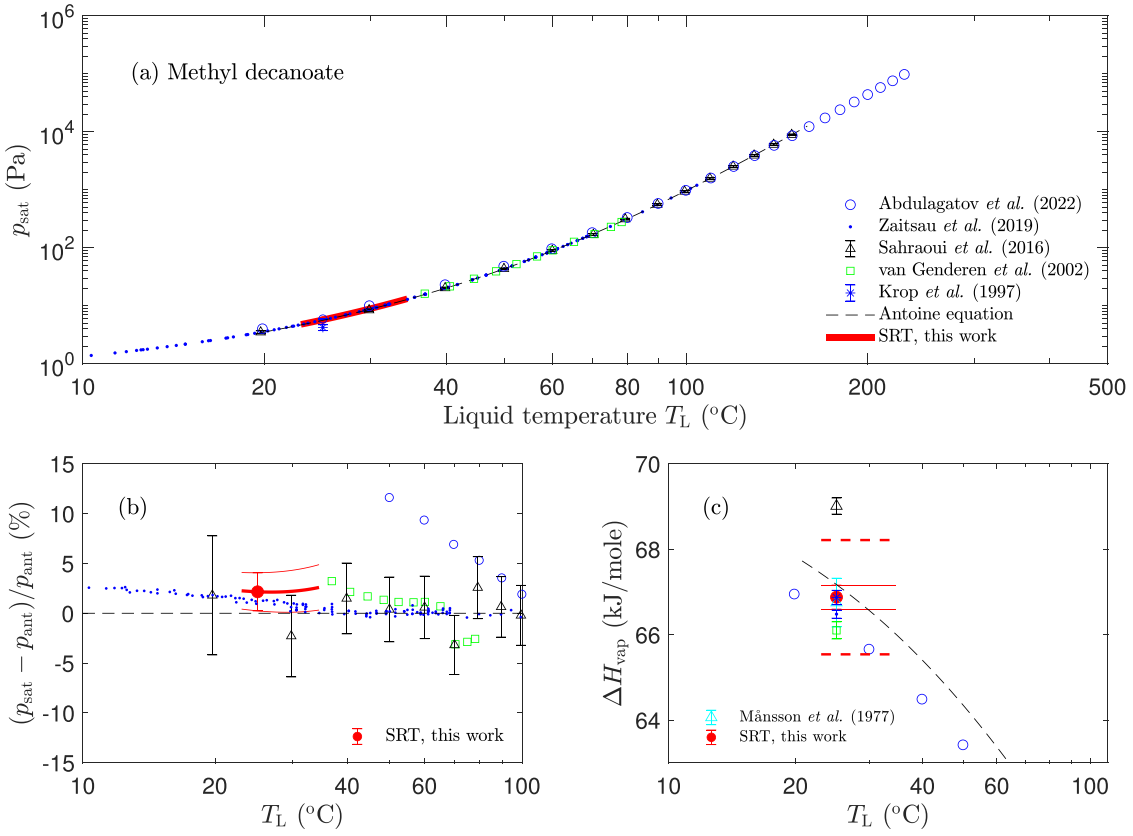

Figure 5. Results of absolute saturation vapor pressure measurements for methyl decanoate and comparison to previous results.[9,12,14−16,34] (a) Saturation vapor pressure as a function of sample temperature. The present data is shown as a red solid line following the form of eq 3 with the fitted values of p^* and ΔH_{vap} from the SRT model (f_{SRT}, eq 1) as given in Table 3. The dashed line shows the Antoine equation established by Sahraoui et al.[15] for the temperature range 20−159 °C. (b) Relative comparison of saturation vapor pressures with the Antoine equation.[15] Note that the Antoine equation is extrapolated outside its nominal temperature range. The red solid lines show the 95% confidence interval of the present measurement. (c) Comparison of the present and previously determined enthalpies of vaporization. The solid red lines indicate the uncertainty from the model fits, while the dashed red lines show the additional 2% uncertainty estimated from the unmodeled temperature dependence of ΔH_{vap}.

6.4.0 program.[31] We used an "energy window (-ewin)" of 30 kcal/mol to ensure that all relevant conformers were sampled. Table 2 presents the identified number of conformers for each of the systems studied using this approach.

For each molecular system, the 1000 conformers of lowest energy at the GFN1-xTB level were subsequently optimized and vibrational frequencies were calculated using density functional theory in Gaussian16, version B.01.[32] We utilized the ωB97X-D[33] density functional with a 6-31++G(d,p) basis set. The vibrational frequencies of the lowest free energy conformer, at 298.15 K and 1 atm, were subsequently selected.

Figure 2 illustrates the calculated vibrational frequencies and also indicates the relative level population at 300 K, i.e., $f_l \propto \exp(-(E_l - E_1)/k_B T)$, where E_l is the energy of the vibrational level l. Around room temperature, only vibrational modes below ∼1000 cm^{-1} are populated, corresponding to delocalized vibrations and C−C vibrations.

2.4. Example of Measurement: Methyl Decanoate. Figure 3 summarizes the saturation vapor determination for methyl decanoate, with Figure 3a,b displaying the sample temperature and chamber pressure observed as a function of time and Figure 3c showing the explicit relation of chamber pressure and sample temperature. Figure 3c also shows fits to the data with the general model (X = SRT, using the vibrational frequencies displayed in Figure 2 for methyl decanoate) and the low-temperature model (X = SVE, D_e = 0). Figure 3d shows the residuals of these fits to scatter around zero, which illustrates the very good representation of the data with the model functions, only marginally favoring the general model over the low-temperature approximation.

A detailed discussion of the various contributions to the uncertainties on the final results of p^* and ΔH_{vap} is given in ref 23. Here, we note explicitly that the applied models assume that the enthalpy of vaporization (ΔH_{vap}) is independent of temperature, which is evidently a simplification. With the limited range of temperatures probed during thermalization for the present measurements, it is, however, not possible to independently account for this variation in the models of the vaporization dynamics. As also discussed previously,[23] the temperature dependence of ΔH_{vap} is expected to amount to ∼2% in the studied temperature range, and, as a consequence, we specify an additional uncertainty on ΔH_{vap} of 2% beyond the uncertainties resulting from the direct measurements of p_V and T_L.

3. RESULTS AND DISCUSSION

Table 3 summarizes the final results of the saturation vapor pressures for the three investigated FAMEs, while Figures 4−6 display the results in comparison with previous measurements. As a basis for the comparison to previous measurements

https://doi.org/10.1021/acsomega.4c08095
ACS Omega 2025, 10, 6671−6678

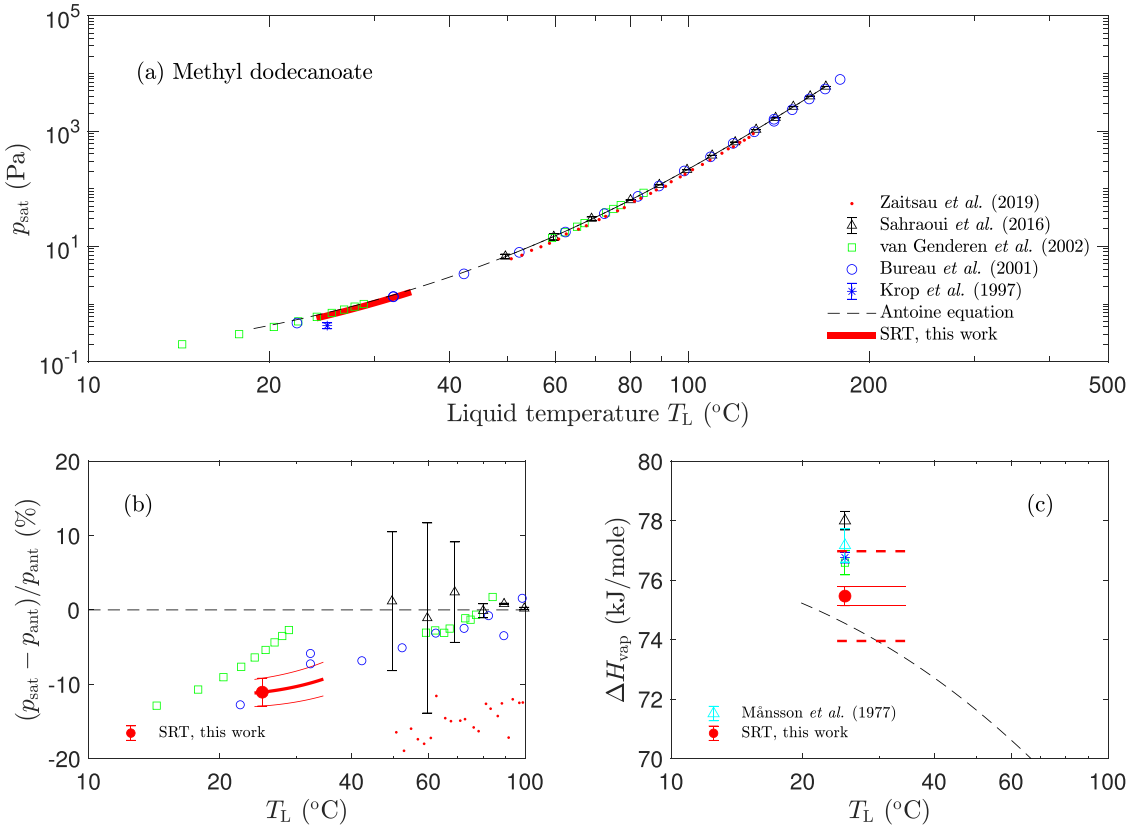

Figure 6. Results of absolute saturation vapor pressure measurements for methyl dodecanoate and comparison to previous results.[9,12−16] The parameters of the Antoine equation are taken from Sahraoui et al.[15] (a) Saturation vapor pressure as a function of sample temperature. The present data is shown as a red solid line following the form of eq 3 with the fitted values of p^* and ΔH_{vap} from the SRT model (f_{SRT}, eq 1) as given in Table 3. The dashed line shows the Antoine equation established by Sahraoui et al.[15] for the temperature range 59.5−169 °C. (b) Relative comparison of saturation vapor pressures with the Antoine equation.[15] Note that the Antoine equation is extrapolated outside its nominal temperature range. The red solid lines show the 95% confidence interval of the present measurement. (c) Comparison of the present and previously determined enthalpies of vaporization. The solid red lines indicate the uncertainty from the model fits, while the dashed red lines show the additional 2% uncertainty estimated from the unmodeled temperature dependence of ΔH_{vap}.

(Figures 4b, 5b, and 6b), we have chosen the Antoine parametrizations given by Sahraoui et al.[15] To predict the temperature variation of the enthalpy of vaporization (Figures 4c, 5c, and 6c), we have computed $\Delta H_{vap}(T)$ from eq 2 using these Antoine parametrizations.

For methyl octanoate (Figure 4), only a single previous measurement[15] (static method) of the saturation vapor pressure covered directly the temperature range investigated here, while another measurement[14] (static method) reported values above 40 °C. As seen from Figure 4b, the saturation vapor pressure reported here agrees well within the specified confidence interval with the previous measurement[15] and probably also with the measurements performed at higher temperatures.[14] With respect to the enthalpy of vaporization for methyl octanoate (Figure 4c), the present measurement is consistent with previous determinations, in particular when considering the unmodeled temperature dependence of ΔH_{vap}.

For methyl decanoate (Figure 5), four previous measurements[12,15,16,34] of the saturation vapor pressure have covered the present temperature range. The present data are consistent with two of these measurements[15,16] (static methods) while the two others[12,34] deviate by more than 20% (Figure 5b). The present determination of the enthalpy of vaporization for methyl decanoate is also consistent with previously reported measurements, as seen in Figure 5c.

For methyl dodecanoate (Figure 6), one previously reported measurement[13] (static method) of the saturation vapor pressure near room temperature compares consistently with the present measurements while a second measurement[14] (effusion method) deviates by ∼5% and a third determination[12] (gas chromatography) deviates strongly (>30%). The presently determined enthalpy of vaporization for methyl dodecanoate also shows consistency with most of the previous measurements (Figure 6c).

The method applied in this work for the determination of saturation vapor pressures is based on a *dynamical* principle, namely, to follow the vaporization dynamics of a sample during thermalization to the higher temperature of a surrounding chamber. This is markedly different from other state-of-the-art methods for absolute saturation pressure determinations which strive to maintain a static gas−liquid equilibrium condition during the measurement. Moreover, the present method provides a continuous range of saturation vapor pressures over the probed temperature range, i.e., the outcome is not limited to specific points where thermal equilibrium has been obtained. Hence, the present results can be considered to be truly complementary to previous measurements.

The present method gives results that support the values of saturation vapor pressures for methyl octanoate given by Sahraoui et al.[15] and van Genderen,[14] for methyl decanoate

https://doi.org/10.1021/acsomega.4c08095
ACS Omega 2025, 10, 6671−6678

given by Sahraoui et al.[15] and Zaitsau et al.,[16] and for methyl dodecanoate given by Bureau et al.[13]

4. CONCLUSIONS

We have reported the measurement of the saturation vapor pressures of three FAMEs with a new dynamic method that is complementary to current state-of-the-art methods.

The applied method works favorably toward lower pressures where the sample does not completely evaporate during preparation, and the method is essentially only limited by the ability to measure absolute pressure. Since we have, in another line of research, developed new absolute pressure sensors with sub-millipascal sensitivity,[35] and instrument developments are ongoing to expand the temperature range that can be probed by the instrument, we expect that accurate saturation vapor pressure and enthalpy of vaporization data will be available for FAMEs and other related additional substances, e.g., in a temperature range below room temperature. From an application perspective, the availability of accurate saturation vapor pressures of FAMEs, as well as other industrial important substances, around or below room temperature can be of significant value in applications in food processing (flavoring) and pharmaceutical productions (e.g., cosmetics). For FAMEs in particular, the optimization of biodiesel engines will clearly benefit from accurate measurements of absolute saturation vapor pressures.

■ ASSOCIATED CONTENT

Supporting Information

The Supporting Information is available free of charge at https://pubs.acs.org/doi/10.1021/acsomega.4c08095.

Figures similar to Figure 3 for methyl decanoate, are provided for methyl octanoate (Figure S1) and methyl dodecanoate (Figure S2) showing the explicit results of the dynamic vaporization measurements during thermalization. (PDF)

■ AUTHOR INFORMATION

Corresponding Author

Henrik B. Pedersen − *Department of Physics and Astronomy, Aarhus University, 8000 Aarhus C, Denmark;* orcid.org/0000-0002-7617-8919; Email: hbp@phys.au.dk

Authors

Mohsen Salimi − *Department of Physics and Astronomy, Aarhus University, 8000 Aarhus C, Denmark*

Jonas Elm − *Department of Chemistry, Aarhus University, 8000 Aarhus C, Denmark*

Aurelien Dantan − *Department of Physics and Astronomy, Aarhus University, 8000 Aarhus C, Denmark;* orcid.org/0000-0003-0441-2873

Complete contact information is available at: https://pubs.acs.org/10.1021/acsomega.4c08095

Notes

The authors declare no competing financial interest.

■ ACKNOWLEDGMENTS

The research was supported by a grant from the Independent Research Fund Denmark (Technology and Production, Grant No. 0136-00345B) and by a grant from the Villum Foundation (Grant No. 50229).

■ REFERENCES

(1) Demirbas, A. Progress and recent trends in biodiesel fuels. *Energy Convers. Manage.* **2009**, *50*, 14−34.

(2) Wedler, C.; Trusler, J. M. Review of density and viscosity data of pure fatty acid methyl ester, ethyl ester and butyl ester. *Fuel* **2023**, *339*, 127466.

(3) Anneken, D. J.; Both, S.; Christoph, R.; Fieg, G.; Steinberner, U.; Westfechtel, A. *Fatty Acids*; John Wiley & Sons Ltd., 2006.

(4) Althouse, P. M.; Triebold, H. O. Physical Constants of Methyl Esters of Commonly Occurring Fatty Acids Vapor Pressure. *Ind. Eng. Chem.* **1944**, *16*, 605−606.

(5) Bonhorst, C. W.; Althouse, P. M.; Triebold, H. O. Esters of Naturally Occurring Fatty Acids - Physical Properties of Methyl, Propyl, and Isopropyl Esters of C6 to C18 Saturated Fatty Acids. *Ind. Eng. Chem.* **1948**, *40*, 2379−2384.

(6) Nevin, C. S.; Althouse, P. M.; Triebold, H. O. Surface tension determinations of some saturated fat acid methyl esters. *J. Am. Oil Chem. Soc.* **1951**, *28*, 325−327.

(7) Scott, T. A.; Macmillan, D.; Melvin, E. H. Vapor pressures and distillation of methyl esters of some fatty acids. *Ind. Eng. Chem.* **1952**, *44*, 172−175.

(8) Rose, A.; Supina, W. R. Vapor Pressure and Vapor-Liquid Equilibrium Data for Methyl Esters of the Common Saturated Normal Fatty Acids. *J. Chem. Eng. Data* **1961**, *6*, 173−179.

(9) Månsson, M.; Sellers, P.; Stridh, G.; Sunner, S. Enthalpies of vaporization of some 1-substituted n-alkanes. *J. Chem. Thermodyn.* **1977**, *9*, 91−97.

(10) Fuchs, R.; Peacock, L. A. Heats of vaporization of esters by the gas chromatography−calorimetry method. *Can. J. Chem.* **1980**, *58*, 2796−2799.

(11) Husain, S.; Sarma, P. N.; Swamy, G. Y. S. K.; Devi, K. S. Determination of physicochemical properties of some fatty acid methyl esters by gas liquid chromatography. *J. Am. Oil Chem. Soc.* **1993**, *70*, 149−155.

(12) Krop, H. B.; van Velzen, M. J. M.; Parsons, J. R.; Govers, H. A. J. Determination of environmentally relevant physical-chemical properties of some fatty acid esters. *J. Am. Oil Chem. Soc.* **1997**, *74*, 309−315.

(13) Bureau, N.; Jose, J.; Mokbel, I.; de Hemptinne, J.-C. Vapour pressure measurements and prediction for heavy esters. *J. Chem. Thermodyn.* **2001**, *33*, 1485−1498.

(14) van Genderen, A. C.; van Miltenburg, J.; Blok, J. G.; van Bommel, M. J.; van Ekeren, P. J.; van den Berg, G. J.; Oonk, H. A. Liquid−vapour equilibria of the methyl esters of alkanoic acids: vapour pressures as a function of temperature and standard thermodynamic function changes. *Fluid Phase Equilib.* **2002**, *202*, 109−120.

(15) Sahraoui, L.; Khimeche, K.; Dahmani, A.; Mokbel, I.; Jose, J. Experimental vapor pressures (from 1 Pa to 100 kPa) of six saturated Fatty Acid Methyl Esters (FAMEs): Methyl hexanoate, methyl octanoate, methyl decanoate, methyl dodecanoate, methyl tetradecanoate and methyl hexadecanoate. *J. Chem. Thermodyn.* **2016**, *102*, 270−275.

(16) Zaitsau, D. H.; Pimerzin, A. A.; Verevkin, S. P. Fatty acids methyl esters: Complementary measurements and comprehensive analysis of vaporization thermodynamics. *J. Chem. Thermodyn.* **2019**, *132*, 322−340.

(17) Abdulagatov, I. M.; Batyrova, R. G.; Polikhronidi, N. G. Simultaneously measurements of vapor-pressure, saturated liquid density, single-phase PVT properties, and thermal -pressure coefficient of methyl decanoate at high- temperatures and high-pressures. *Fluid Phase Equilib.* **2022**, *560*, 113506.

(18) Spieksma, W.; Luijk, R.; Govers, H. A. Determination of the liquid vapour pressure of low-volatility compounds from the Kováts retention index. *J. Chromatogr. A* **1994**, *672*, 141−148.

(19) Kasehgari, H.; Mokbel, I.; Viton, C.; Jose, J. Vapor pressure of 11 alkylbenzenes in the range 0.001 - 280 Torr, correlation by equation of state. *Fluid Phase Equilib.* **1993**, *87*, 133−152.

(20) Verevkin, S. P.; Emel'yanenko, V. N. Transpiration method: Vapor pressures and enthalpies of vaporization of some low-boiling esters. *Fluid Phase Equilib.* **2008**, *266*, 64−75.
(21) Widegren, J. A.; Harvey, A. H.; McLinden, M. O.; Bruno, T. J. Vapor Pressure Measurements by the Gas Saturation Method: The Influence of the Carrier Gas. *J. Chem. Eng. Data* **2015**, *60*, 1173−1180.
(22) Chickos, J. S.; Acree, J.; William, E. Enthalpies of Vaporization of Organic and Organometallic Compounds, 1880−2002. *J. Phys. Chem. Ref. Data* **2003**, *32*, 519−878.
(23) Nielsen, R. V.; Salimi, M.; Andersen, J. E. V.; Elm, J.; Dantan, A.; Pedersen, H. B. A new setup for measurements of absolute saturation vapor pressures using a dynamical method: Experimental concept and validation. *Rev. Sci. Instrum.* **2024**, *95*, 065007.
(24) Fang, G.; Ward, C. A. Examination of the statistical rate theory expression for liquid evaporation rates. *Phys. Rev. E* **1999**, *59*, 441−453.
(25) Persad, A. H.; Ward, C. A. Expressions for the Evaporation and Condensation Coefficients in the Hertz-Knudsen Relation. *Chem. Rev.* **2016**, *116*, 7727−7767.
(26) Kazemi, M. A.; Ward, C. A. Assessment of the statistical rate theory expression for evaporation mass flux. *Int. J. Heat Mass Transfer* **2021**, *179*, 121709.
(27) Grimme, S. Exploration of Chemical Compound, Conformer, and Reaction Spacewith Meta-Dynamics Simulations Based on Tight-Binding QuantumChemical Calculations. *J. Chem. Theory Comput.* **2019**, *15*, 2847−2862.
(28) Pracht, P.; Bohle, F.; Grimme, S. Automated Exploration of the Low-energy Chemical Space with Fast Quantum Chemical Methods. *Phys. Chem. Chem. Phys.* **2020**, *22*, 7169−7192.
(29) Pracht, P.; Grimme, S.; Bannwarth, C.; Bohle, F.; Ehlert, S.; Feldmann, G.; Gorges, J.; Müller, M.; Neudecker, T.; Plett, C.; Spicher, S.; Steinbach, P.; Wesołowski, P. A.; Zeller, F. CREST—A Program for the Exploration of Low-energy Molecular Chemical Space. *J. Chem. Phys.* **2024**, *160*, 114110.
(30) Grimme, S.; Bannwarth, C.; Shushkov, P. A Robust and Accurate Tight-Binding Quantum Chemical Method for Structures, Vibrational Frequencies, and Noncovalent Interactions of Large Molecular Systems Parametrized for All spd-Block Elements (Z = 1−86). *J. Chem. Theory Comput.* **2017**, *13*, 1989−2009.
(31) Bannwarth, C.; Caldeweyher, E.; Ehlert, S.; Hansen, A.; Pracht, P.; Seibert, J.; Spicher, S.; Grimme, S. Extended Tight-binding Quantum Chemistry Methods. *WIREs Comput. Mol. Sci.* **2021**, *11*, e1493.
(32) Frisch, M. J.; Trucks, G. W.; Schlegel, H. B.; Scuseria, G. E.; Robb, M. A.; Cheeseman, J. R.; Scalmani, G.; Barone, V.; Petersson, G. A.; Nakatsuji, H.et al. *Gaussian 16, Revision B.01*; Gaussian, Inc.: Wallingford, CT, 2016.
(33) Chai, J.-D.; Martin, H. Long-Range Corrected Hybrid Density Functionals with Damped Atom-Atom Dispersion Corrections. *Phys. Chem. Chem. Phys.* **2008**, *10*, 6615−6620.
(34) Abdulagatov, I. M.; Polikhronidi, N. G.; Batyrova, R. G.; Dzida, M. Isochoric heat capacity, phase transition and derived key thermodynamic properties of methyl decanoate. *Fuel* **2022**, *310*, 122251.
(35) Salimi, M.; Nielsen, R. V.; Pedersen, H. B.; Dantan, A. Squeeze film absolute pressure sensors with sub-millipascal sensitivity. *Sens. Actuators, A* **2024**, *374*, 115450.

https://doi.org/10.1021/acsomega.4c08095
ACS Omega 2025, 10, 6671−6678